Hydrodynamic stability of three-dimensional homogeneous flow topologies

Aashwin A. Mishra* and Sharath S. Girimaji
Department of Aerospace Engineering, Texas A&M University, College Station, Texas 77843-3141, USA
(Received 10 July 2014; published 2 November 2015)

This article examines the hydrodynamic stability of various homogeneous three-dimensional flow topologies. The influence of inertial and pressure effects on the stability of flows undergoing strain, rotation, convergence, divergence, and swirl are isolated. In marked contrast to two-dimensional topologies, for three-dimensional flows the inertial effects are always destabilizing, whereas pressure effects are always stabilizing. In streamline topologies with a negative velocity-gradient third invariant, inertial effects prevail leading to instability. Vortex-stretching is identified as the underlying instability mechanism. In flows with positive velocity-gradient third derivative, pressure overcomes inertial effects to stabilize the flow.

DOI: 10.1103/PhysRevE.92.053001 PACS number(s): 47.20.Cq, 47.11.−j, 47.27.Ak, 47.27.Cn

The stability of three-dimensional flows under the joint effects of strain and rotation is of intrinsic importance in diverse fields. In air transport, trailing vortices pose grave hazards to aircraft [1]. Similarly, elliptic streamline flows pose a long-standing challenge in turbulence modeling [2]. The existence of stable vortices in strongly turbulent planetary atmospheres, such as the Great Red Spot on Jupiter, is a challenging problem in astrophysics [3,4]. In this vein, the most elementary flows exhibiting innate instabilities are homogeneous flows subjected to spatially uniform deformation. In literature, stability analyses of homogeneous flows employ two distinct approaches: *hydrodynamic stability* and *rapid distortion theory* (RDT). The geometric approach to hydrodynamic stability was pioneered by Arnold [5] and further developed by Friedlander and coworkers [6–8]. Using this technique, Friedlander and Vishik [6] have proved that all planar homogeneous flows with hyperbolic stagnation points are unstable. Their system of equations, circumscribing the growth rate of the Green's function evolution operator, are exactly equivalent to the Kelvin-Moffat system [9] used in RDT-based investigations. As observed in Cambon [10], RDT examines *both the transients and the asymptotic states of the flow*. Cambon [10] employed this approach to analyze the elliptic flow instability. Subsequently, the stability of planar flows with uniform gradients has been extensively examined by Cambon and coworkers [11–13] and other investigators [14–16]. At the interface of the geometric hydrodynamic stability and the RDT-based approaches are investigations such as those of Craik and Criminale [17], Waleffe [18], and Bayly [19].

While homogeneous flows are, in principle, amenable to a unified treatment, only flows undergoing two-dimensional (planar) deformations have hitherto been examined in detail in literature. In spite of the fact that three-dimensional flows include important cases such as flows with swirl and axisymmetric expansion and contraction, the stability, dynamics, and evolution of these flows have not been analyzed as extensively. The primary objective of this article is *to investigate the linear stability of specific three-dimensional flows*. To this end, we aim to *isolate and explicate the role of the inertial and pressure effects on flow stability*.

*aashwin@tamu.edu

A significant amount of work has also been conducted on the topological characterization of velocity gradient evolution in turbulent flows [20–22]. This line of analysis focuses on the nonlinear interactions of the fluctuating velocity field, in the absence of any influence of the mean flow. The focus of our investigation is on the effect of spatially uniform mean flows on the linear dynamics of perturbation evolution. Homogeneous background flows are characterized in terms of the velocity gradients

$$A_{ij} = \frac{\partial U_i}{\partial x_j}, \quad S_{ij} = \frac{A_{ij} + A_{ji}}{2}, \quad W_{ij} = \frac{A_{ij} - A_{ji}}{2}, \quad (1)$$

where A_{ij}, S_{ij}, and W_{ij} are the velocity gradient, strain rate, and rotation rate tensors. A general three-dimensional background velocity gradient field can be represented as

$$A_{ij} = \begin{bmatrix} \sigma_1 & \omega_3 & \omega_2 \\ -\omega_3 & \sigma_2 & \omega_1 \\ -\omega_2 & -\omega_1 & -\sigma_1 - \sigma_2 \end{bmatrix}. \quad (2)$$

This background velocity gradient field is maintained spatially and temporally uniform with the application of appropriate body forces [23]. For an incompressible flow, the first (P), second (Q), and third (R) invariants of the velocity gradient tensor are

$$P = \mathrm{tr}(A) = 0;$$
$$Q = -\frac{\mathrm{tr}(AA^T)}{2} = -\left(\sigma_1^2 + \sigma_2^2 + \sigma_1\sigma_2 + \omega_1^2 + \omega_2^2 + \omega_3^2\right);$$
$$R = -\det(A) = (\sigma_1 + \sigma_2)\left(\sigma_1\sigma_2 + \omega_3^2\right) - \left(\sigma_1\omega_1^2 + \sigma_2\omega_2^2\right).$$

For incompressible flows, P, representing the additive inverse of the dilatation is zero. In compressible flows, a nonzero value of P signifies the degree of compression and expansion in the mean flow. The second and the third invariants provide information regarding the mean flow topology. If the mean velocity gradient is normalized by its norm, $a_{ij} = \frac{A_{ij}}{\sqrt{A_{mn}A_{mn}}}$, the corresponding invariants of the normalized tensor, (p, q, r), can be bounded as $p \in [-\sqrt{3}, \sqrt{3}]$, $q \in [\frac{-1}{2}, 1]$, and $r \in [\frac{-1}{3\sqrt{3}}, \frac{1}{3\sqrt{3}}]$. The streamline topology of the background flow can be categorized on the basis of Q and R as shown in Fig. 1. The $R = 0$ line corresponds to planar background flows: $Q > 0$ represents elliptic streamline flows; $Q < 0$ represents hyperbolic streamline flows; and $Q = R = 0$ represents a

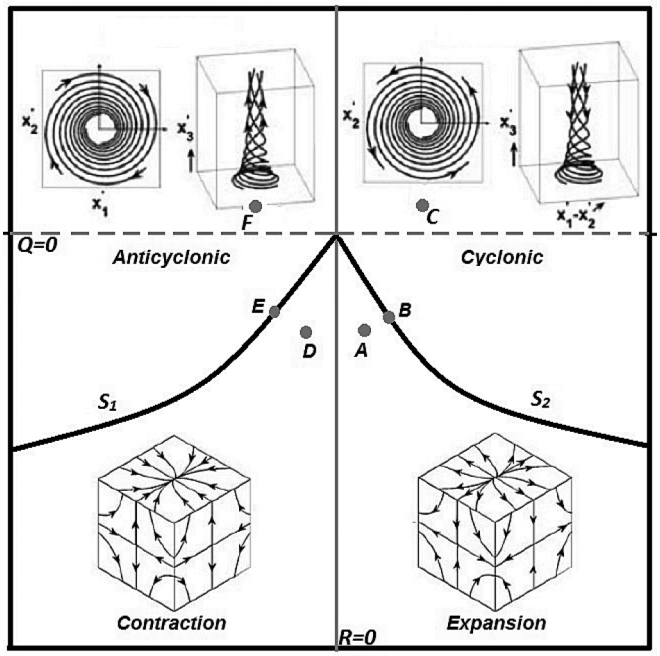

FIG. 1. Classification of flow regimes with respect to Q and R.

planar purely sheared flow. The curves S_1 and S_2, representing solutions of $27R^2 + 4Q^3 = 0$, separate zones of real and complex roots for the local flow topology. For $R \neq 0$, we follow Chong *et al.* [24] to categorize the topologies. Expansion ($R > 0$, $Q < S_2$) and Contraction ($R < 0$, $Q < S_1$) flows are topologically homeomorphic to their axisymmetric counterparts. Thus, the benchmark cases of axisymmetric contraction and axisymmetric expansion flows would lie on the lines marked S_1 and S_2 in the figure. The Cyclonic ($R > 0$, $Q > S_2$) and the anticyclonic ($R < 0$, $Q > S_1$) flows reflect the directionality of swirl [25]. The interested reader is referred to Ref. [26], wherein a comparison of such idealized streamlines and their realization in nature is shown.

Prior studies on planar background flows have demonstrated that linear stability is a topological property and, thus, is strongly dependent on the structure of the streamlines of the background flow [13–16]. Therefore, to study the stability of a specific background flow topology, it may be adequate to examine a small set of representative velocity gradients. In this investigation, we restrict the analysis to the case wherein the vorticity axis vector coincides with the three-axis of the coordinate system. The one and two axes are taken to coincide along the strain rate eigendirections on the plane of rotation. Thus, the mean gradient reduces to

$$A_{ij} = \begin{bmatrix} \sigma_1 & \omega & 0 \\ -\omega & \sigma_2 & 0 \\ 0 & 0 & -\sigma_1 - \sigma_2 \end{bmatrix}. \quad (3)$$

This subset of the general three-dimensional case enables systematic classification and analysis. Additionally, this subset still contains benchmark flows such as those with expansion, contraction, and swirl.

The rapid distortion equations in dimensional form, for the velocity perturbation ($\vec{u}'$) subjected to a given mean velocity field, are given by [9]

$$\frac{\bar{D}u'_j}{\bar{D}t} = -u'_i \frac{\partial U_j}{\partial x_i} - \frac{1}{\rho}\frac{\partial p}{\partial x_j}, \quad \frac{1}{\rho}\nabla^2 p = -2\frac{\partial U_j}{\partial x_i}\frac{\partial u'_i}{\partial x_j}. \quad (4)$$

Here, the $\frac{\bar{D}}{\bar{D}t}$ operator represents the total derivative following a mean streamline. These equations are examined in Fourier space, via the projection: $u'_i(\mathbf{x},t) = \sum u_i(\boldsymbol{\kappa},t)e^{i\boldsymbol{\kappa}\cdot\mathbf{x}}$, $p(\mathbf{x},t) = \sum \hat{p}(t)(\boldsymbol{\kappa},t)e^{i\boldsymbol{\kappa}\cdot\mathbf{x}}$. The evolution equations in Fourier space are

$$\frac{du_j}{dt} = u_k A_{lk}(2e_j e_l - \delta_{jl}), \quad \frac{de_l}{dt} = e_m A_{mi}(e_i e_l - \delta_{il}), \quad (5)$$

subject to the orthogonality condition, $u_i e_i = 0$. Here, $\vec{u}$ and $\vec{e}$ represent the Fourier amplitude and the unit wave-number vectors ($\vec{e} = \frac{\vec{\kappa}}{|\kappa|}$). The Fourier amplitude evolution is governed by

$$\frac{du_\alpha u^*_\alpha}{dt} = -(u_k u^*_\alpha + u^*_k u_\alpha)A_{\alpha k} + 2A_{lk}e_l e_\alpha (u_k u^*_\alpha + u^*_k u_\alpha), \quad (6)$$

where the Greek indices are independent of the summation convention and * represents the complex conjugate. The amplitude evolution is dictated by two distinct processes. First is the inertial *production mechanism*, $P_{\alpha\alpha} = -(u_k u^*_\alpha + u^*_k u_\alpha)A_{\alpha k}$. The *pressure redistribution mechanism*, $\pi_{\alpha\alpha} = 2A_{lk}e_l e_\alpha (u_k u^*_\alpha + u^*_k u_\alpha)$, modifies the velocity amplitude to preserve $u_i e_i = 0$ and is contingent upon the wave-vector alignment.

To isolate and analyze the role of the mechanisms in the evolution of the flow, we utilize the technique of Burgulence [9]. Herein, the evolution of a "pressure-released" Burgers system is contrasted against the Euler system to isolate the effects of inertia and pressure. For planar background flows, the dependence of the inertial and pressure effects, along with stability, upon the flow topology is summarized in Table I.

For each representative background flow considered, we analyze the kinetic energy evolution of over 12 000 perturbation modes, distributed uniformly on a unit sphere in wave-vector space, as an ensemble, as well as individual modes in isolation. A fourth-order Runge-Kutta scheme was used for temporal integration of all equations. For additional details of the solution procedure, the interested reader is referred to Mishra [27,28]. The stability of the flow is inferred from the kinetic energy evolution of the ensemble and the underlying dynamics are explained in terms of the wave-vector evolution. The analysis is carried out for disparate ensembles and for different flow topologies spanning the parameter space. Utilizing the homeomorphic nature of flow topologies within a regime and the observed similitude in their evolution, we present specific representative cases. Hereon, the analysis considers the dynamics in the flow topologies, individually.

TABLE I. Inertial effects, pressure effects, and flow stability for planar homogeneous flow topologies.

Flow	Inertial Effects	Pressure Effect	Overall Stability
Hyperbolic	Destabilizing	Stabilizing	Unstable
Pure shear	Destabilizing	Mildly stabilizing	Unstable
Elliptic	*Neutral*	*Destabilizing*	Unstable

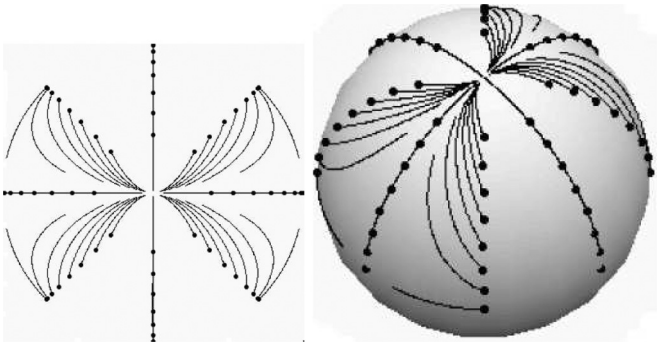

FIG. 2. Expansion flows: Unit wave-number vector evolution from a set of initial conditions marked by dark circles. Left: The e_1-e_2 plane projection. Right: Unit wave-vector sphere with equatorial plane representing the 1−2 plane.

Expansion flows. In Fig. 1, a typical expansion flow is given by point A, $(R, Q) = (0.087, -0.99)$. In such flows, the one- and two-axes have negative production of perturbation energy while the three-axis has positive production. The inertial effects engender a state of exponential instability with the energy resident in the u_3 component. However, as seen in Fig. 2, almost all wave vectors in the flow are attracted to the three-axis. Thus, the inertial effects produce energy for the u_3 component and the wave vectors are aligning with the three-axis ($e_3 \to 1$). To maintain $u_i e_i = 0$, pressure effects transfer perturbation kinetic energy from the u_3 component to the u_1 and u_2 components. This energy redistribution arrests the positive production along the three-axis *and* the transferred energy is consumed by negative production. This leads to a state of asymptotic stability, as exhibited in Fig. 3.

Cyclonic flows. In Fig. 1, a representative cyclonic flow case is given by point C, $(R, Q) = (0.87, 0.5)$. In a cyclonic flow,

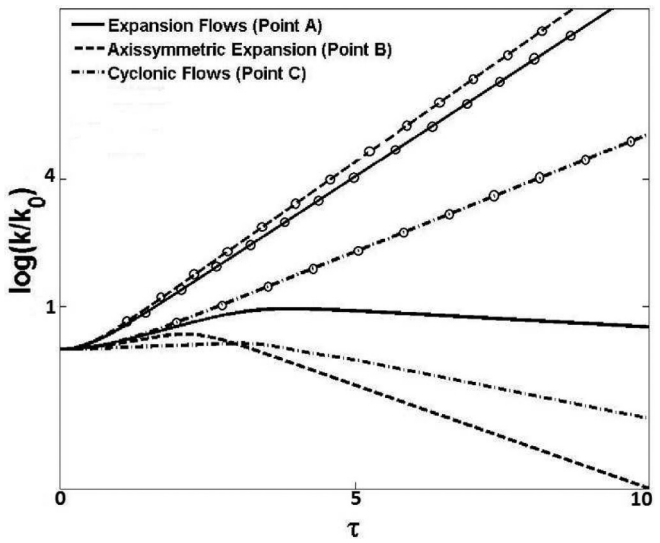

FIG. 3. Perturbation kinetic energy evolution of RDT (lines) and corresponding Burgers (marked with circles) systems, for background flows wherein $R > 0$. τ represents time, normalized with the magnitude of the background velocity gradient, the natural logarithm is plotted.

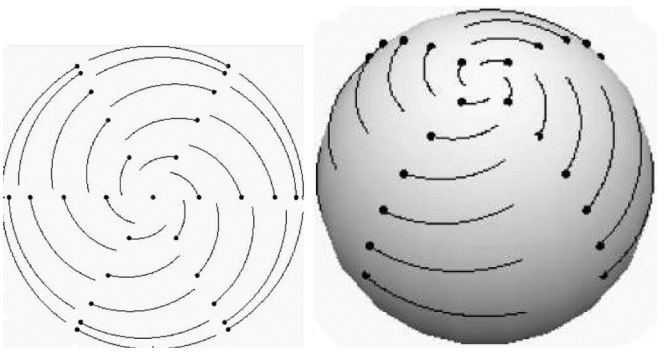

FIG. 4. Cyclonic flows: Unit wave-number vector evolution. (See Fig. 2 for legend.)

the inertial effects lead to a state of exponential instability. The one- and two-axes have a negative production and the three-axis has a positive production. Thus, perturbation kinetic energy is resident in the u_3 component. Considering the phase space of the unit wave-number vector, all the wave vectors are attracted to the limit cycle at $e_3 = 1$, along helical trajectories (Fig. 4). Consequently, the inertial effects produce energy for the u_3 component *and* the wave vectors are aligning with the three-axis ($e_3 \to 1$). Here, the pressure effects transfer perturbation kinetic energy from the u_3 component to the u_1 and u_2 components. This energy redistribution arrests the positive production along the three-axis. The transferred energy is consumed by negative production along the one- and the two-axes. This leads to a state of asymptotic stability, as seen in Fig. 3.

In summary, for flows with a positive third invariant ($R > 0$) we have

(1) Production: P_{11}, $P_{22} \leqslant 0$; $P_{33} > 0$

(2) Redistribution: From $u_3 u_3^*$ to $u_1 u_1^*$, $u_2 u_2^*$.

In expansion and cyclonic flows, the pressure-released case is unstable due to the mechanism of vortex stretching along the axis of rotation. However, the perturbation energy redistribution due to pressure, along with the ensuing negative production, obviates the vortex stretching mechanism leading to a state of flow stability.

Anticyclonic flows. In Fig. 1, an instance of such flows is given by point F, $(R, Q) = (-0.87, 0.5)$. In such flows, the inertial effects engender a state of exponential instability with the perturbation kinetic energy resident in the u_1 and u_2 components. However, all the modal alignments are attracted to the limit cycle in the 1–2 plane, as observed in Fig. 5. To maintain continuity, pressure effects manifest different inter-component energy redistribution for modes with large e_3, as opposed to modes with small e_3. (i) When e_3 is large, pressure transfers energy from the fluctuations in the 1−2 plane to that along the three-axis. This transfer occurs during the migration of the unit wave-vector trajectories to the limit cycle. If the pressure effects are able to completely drain the fluctuations in the 1−2 plane before this state is reached, the mode is stable. Once the unit wave-number vector is close to the 1–2 plane (small e_3), pressure dynamically redistributes energy among the u_1 and the u_2 components in accordance with e_1-e_2 evolution to preserve the incompressibility condition. Depending upon the mode, the pressure redistribution may or

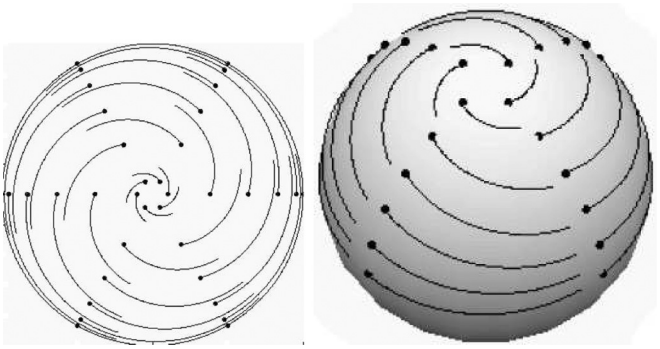

FIG. 5. Anticyclonic flows: Unit wave-number vector evolution. (See Fig. 2 for legend.)

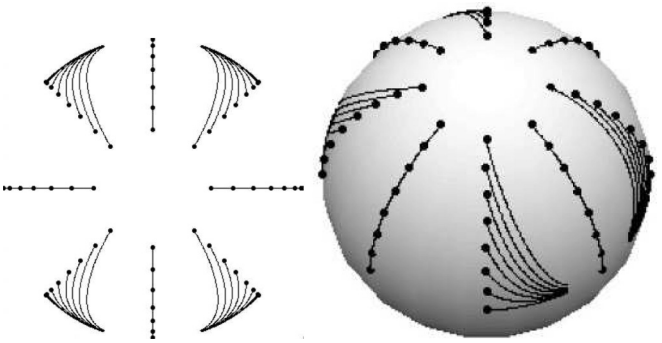

FIG. 7. Contraction flows: Unit wave-number vector evolution. (See Fig. 2 for legend.)

may not completely offset inertial effects. As can be seen in Fig. 6, overall pressure has a mildly stabilizing effect. After an initial period of pressure stabilization, the inertial effects prevail and flow is exponentially unstable.

Contraction flows. In Fig. 1, a representative case of contraction flows is given by the point D, $(R, Q) = (-0.087, -0.99)$. Here, the inertial effects lead to a state of exponential instability with the perturbation kinetic energy produced in the fluctuations along the $1-2$ plane. All modal alignments evolve to stationary states in the e_1-e_2 plane, as exhibited in Fig. 7. At early times, when e_3 is large, pressure transfers energy from the fluctuations in the $1-2$ plane to those along three-axis. At later times (small e_3), when both the velocity and wave vectors are confined to the neighborhood of the $1-2$ plane, production is reduced due to the energy redistribution due to pressure. Due to the nature of this energy redistribution, all modes are not stabilized by pressure effects. Beyond this transient, the inertial effects prevail and flow remains unstable (Fig. 6).

In summary, for flows with a positive third invariant ($R > 0$) we have

(1) Production: $P_{11}, P_{22} \geqslant 0;\ P_{33} < 0$

(2) Redistribution: From $u_1u_1^*, u_2u_2^*$ to $u_3u_3^*$.

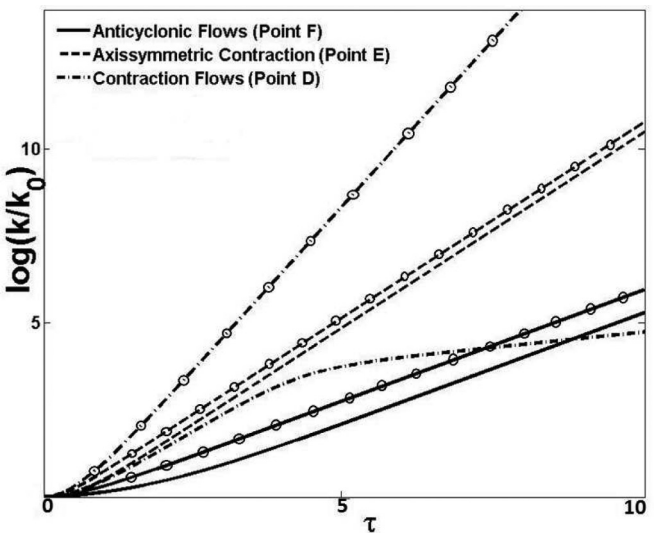

FIG. 6. Perturbation kinetic energy evolution of RDT (lines) and corresponding Burgers (marked with circles) systems, for background flows wherein $R < 0$. The natural logarithm is plotted.

In contraction and anticyclonic flows, the pressure-released flow is unstable due to the mechanism of vortex stretching. The perturbation energy redistribution due to pressure counteracts this mechanism for *some modes only* and *moderates* the rate of instability growth. However, the flow instability and the vortex stretching mechanism persist.

Planar flows (with $R = 0$) form the bifurcation boundary in Q-R parameter space, between stable and unstable three-dimensional flows. Planar hyperbolic flows present a natural transition between the behavior observed in three-dimensional expansion and contraction flows. However, for planar elliptic flows, *in contrast to all the other flow topologies*, the inertial effects engender a state of neutral stability while the pressure effects actually initiate and sustain the flow instability. As can be observed from Tables I and II, the action of the inertial and pressure effects in this regime are *markedly different* from all other flows. Additionally, characteristic phenomena like that of *parametric resonance* underlying the elliptic flow instability, are found to be completely absent in the three-dimensional rotation-dominated flows analyzed. In this vein, *the case of elliptic flows may represent a singular limit*. The results of this study address the underlying linear physics. To gauge their applicability to nonlinear fluid dynamics, the interested reader is referred to Mishra and Girimaji [29], Lee *et al.* [30]

In conclusion, we demonstrate that the inertial effects, the action of pressure, and the overall stability in certain three-dimensional homogeneous flows is dependent upon the third invariant of the velocity gradient. Herein, *flows where the flow topology has a positive value of the third invariant ($R > 0$) are stable, while flows where $R < 0$ are unstable*. For such

TABLE II. Inertial effects, pressure effects, and flow stability of nonplanar homogeneous flow topologies

Flow	Inertial Effects	Pressure Effect	Overall Stability
Expansion ($R > 0$)	Destabilizing	Stabilizing	Stable
Cyclonic ($R > 0$)	Destabilizing	Stabilizing	Stable
Anticyclonic ($R < 0$)	Destabilizing	Mildly stabilizing	Unstable
Contraction ($R < 0$)	Destabilizing	Mildly stabilizing	Unstable

three-dimensional flows, the inertial effects are destabilizing and lead to a state of exponential instability. The effect of pressure has a stabilizing influence on such three-dimensional topologies. In flow topologies with $R > 0$, pressure effects are able to dominate and lead to flow stability. For flows with $R < 0$, the inertial effects dominate and the flow remains unstable.

[1] P. Spalart, Annu. Rev. Fluid Mech. **30**, 107 (1998).
[2] C. Cambon and J. F. Scott, Annu. Rev. Fluid Mech. **31**, 1 (1999).
[3] P. Marcus, Nature **331**, 693 (1988).
[4] J. Sommeria, S. Meyers, and H. Swinney, Nature **331**, 689 (1988).
[5] V. Arnold, *Topological Methods in Hydrodynamics* (Springer, Berlin, 1999).
[6] S. Friedlander and M. M. Vishik, Phys. Rev. Lett. **66**, 2204 (1991).
[7] S. Friedlander and M. Vishik, Chaos **2**, 455 (1992).
[8] S. Friedlander, A. D. Gilbert, and M. Vishik, Geophys. Astrophys. Fluid Dynam. **73**, 97 (2006).
[9] P. Sagaut and C. Cambon, *Homogeneous Turbulence Dynamics* (Cambridge University Press, Cambridge, 2008).
[10] C. Cambon, "Étude spectrale d'un champ turbulent incompressible, soumis à des effets couplés de déformation et de rotation, imposés extérieurement" (1982), thèse de Doctorat d'État, Université de Lyon, France.
[11] L. Jacquin, O. Leuchter, C. Cambon, and J. Mathieu, J. Fluid Mech. **220**, 1 (1990).
[12] C. Cambon and L. Jacquin, J. Fluid Mech. **202**, 295 (1989).
[13] A. Salhi, C. Cambon, and C. Speziale, Phys. Fluids **9**, 2300 (1997).
[14] A. Mishra and S. Girimaji, Flow, Turbul. Combust. **85**, 593 (2010).
[15] A. Mishra and S. Girimaji, J. Fluid Mech. **731**, 639 (2013).
[16] A. Mishra and S. Girimaji, J. Fluid Mech. **755**, 535 (2014).
[17] A. D. D. Craik and W. O. Criminale, Proc. R. Soc. London A **406**, 13 (1986).
[18] F. Waleffe, Phys. Fluids A: Fluid Dynam. **2**, 76 (1990).
[19] B. J. Bayly, Phys. Rev. Lett. **57**, 2160 (1986).
[20] P. Vieillefosse, J. Phys. **43**, 837 (1982).
[21] C. Meneveau, Annu. Rev. Fluid Mech. **43**, 219 (2011).
[22] S. Suman and S. Girimaji, J. Fluid Mech. **683**, 289 (2011).
[23] H. Yu and S. S. Girimaji, Phys. Fluids **17**, 125106 (2005).
[24] M. Chong, A. Perry, and B. Cantwell, Phys. Fluids **2**, 765 (1990).
[25] I. Tannehill, Publication No. 197: The Hurricane (U.S. Department of Agriculture, 1934).
[26] G. Haller, Annu. Rev. Fluid Mech. **47**, 137 (2015).
[27] A. Mishra, "A dynamical systems approach towards modeling the rapid pressure strain correlation" (2010), Master of Science Thesis, Texas A & M University, College Station, TX.
[28] A. Mishra, The art and science in modeling the pressure-velocity interactions, Ph.D. thesis, Texas A&M University, College Station, TX, 2014.
[29] A. Mishra and S. Girimaji, ERCOFTAC Bull. **92**, 11 (2012).
[30] M. J. Lee, J. Kim, and P. Moin, J. Fluid Mech. **216**, 561 (1990).